The Impact of Cirrus Clouds on Retrieval of Ozone in the Upper Troposphere / Lower Stratosphere from SMILES Data

Jana MENDROK, Philippe BARON, and KASAI Yasuko

Characterized by an exceptionally low instrumental noise, tropospheric measurements of the Superconducting Submillimeter-Wave Limb Emission Sounder (SMILES), dedicated to the observation of atmospheric ozone chemistry, may noticeably be affected by cirrus clouds. When not taken into account in the retrieval, the change in broadband spectral signal caused by ice clouds introduces uncertainties in the derivation of trace gas profiles around the upper troposphere / lower stratosphere (UTLS). In this paper, we demonstrate cirrus effects on sub-mm limb spectra as well as on the measurement sensitivity concerning trace gas profile retrievals. We analyze the error budget in the retrieval of UTLS ozone (O_3) induced by neglecting the observed cirrus. Furthermore, possibilities to compensate for cloud effects by retrieving additional parameters like a measurement baseline and (pseudo) water vapor (H_2O) content are evaluated.

1 Introduction

Within the last decade, a number of satellite sub-mm limb sounding missions has been developed with Odin/SMR[10] and EOS-MLS[17] among them now operating successfully for several years. While focused on measuring atmospheric trace gase profiles, frequent observations of upper tropospheric ice clouds by these instruments are expected according to previous studies[3][5] and have recently been demonstrated in the measurements[6][18]. This sensitivity to ice clouds, that is supported by the very long path lenghts through atmospheric layers characteristic for limb measurements, facilitates the detection of cirrus and the retrieval of cloud properties. On the other hand, the "contamination" of molecular emission and absorption spectra by clouds complicates trace gas retrievals. Although a number of radiative transfer forward models are capable of considering ice clouds, especially of their scattering features, atmospheric profiles are usually retrieved assuming clear-sky conditions (first attempts of retrievals from cloudy measurements have just recently been presented by Ekström et al.[4]). That means, not taken into account in the inversion procedure, cloud effects on measured signal introduce uncertainties and errors in the estimation of the atmospheric profiles.

In comparison to the aforementioned operating missions, the SMILES instrument, planned to be operated on the Japanese Experimental Module (JEM) of the International Space Station (ISS) from the year 2009, fea-

tures an exceptionally low instrumental noise, i.e., a very high sensitivity of the measurements. SMILES has been designed to measure trace gas species that are important for a detailed understanding of atmospheric chemistry related to ozone destruction. Its high sensitivity will allow the observation of trace gases having weak spectroscopic signatures. Beside that, effects of thin upper tropospheric ice clouds can easiliy be larger than the instrumental noise and become noticeable in the measurements. That may facilitate the detection of ice clouds in the UTLS, which are supposed to increase the efficiency of chemical processes leading to ozone loss. On the other hand, the effects of clouds on the measured spectra also cause uncertainties in the retrieval of UTLS trace gas profiles.

Within this work we analyse the error budget, that is introduced by not accounting for ice clouds in the retrieval of UTLS profiles of ozone. For that, SMILES observations of a wide variety of cirrus clouds are simulated by the radiative transfer model SARTre[9], which is capable to model scattering of microwave radiation in a spherical atmosphere. From the simulated measurements profile retrievals of ozone are performed using the MOLIERE radiative transfer forward and inversion model[16]. The error budget introduced by cirrus is evaluated.

In section **2**, the models used for simulating SMILES observations and for inversion are described along with the setup of the study and the parameters of the SMILES instruments. Sections **3** and **4** will discuss the effect of cirrus clouds on SMILES limb observations and on retrieval sensitivity quantitatively described by weighting functions. In section **5** the implications of cirrus occurence in the observations for retrieval of ozone profiles are presented. Furthermore, possibilities to account for clouds and improve O₃ profile retrievals are evaluated. Finally, section **6** gives a summary on the study results and draws conclusions.

2 Method and data

2.1 The SMILES instrument

SMILES will measure limb emission spectra in three single side band filtered bands between 624.32–650.32 GHz (but only two of them simultaneously) with a spectral resolution of 1.8 MHz and a spacing of 0.8 MHz. The atmosphere will be nominally scanned from tangent altitudes of −10 km to approximately 100 km, ensuring the coverage of altitudes between 10–80 km despite uncertainties and instabilities of the ISS attitude. With a beam width of 0.096° and a sampling interval of 0.056°, the field of view of a single limb measurement is approximately 4 km wide at the tangent point and the vertical spacing between two subsequent measurements is about 2 km[13].

One of the most unique characteristics of JEM/SMILES will be its exceptionally low system temperature of 500 K giving a thermal noise of only 0.5 K for an integration time of 0.5 s for a single measurement. This high sensitivity allows the observation of trace gas species that have only weak spectroscopic signatures. Table 1 gives an overview of the SMILES spectral bands and the target species, that will be retrieved from the individual bands.

While the instrument's high sensitivity allows for improved retrievals of species with weak spectral signature in the mesosphere and stratosphere, lower stratospheric and upper tropospheric spectra may be measureably affected by ice clouds. On the one hand that

Table 1 *SMILES band characteristics*

Band	Spectral Coverage	Target Species
A	624.32 – 625.52 GHz	O_3, O_3-isotopes, $H^{37}Cl$, H_2O_2, $HO^{35}Cl$, HNO_3, SO_2, ^{81}BrO
B	625.12 626.32 GHz	O_3, O_3-isotopes, $H^{35}Cl$, HO_2, HNO_3, SO_2, $O^{35}ClO$
C	649.12 – 650.32 GHz	^{35}ClO, O_3-isotopes, HO_2, HNO_3, SO_2, ^{81}BrO

may facilitate the detection and characterization of ice clouds that play an important role in the global energy balance and water cycle. Being supposed to increase the efficiency of chemical processes leading to ozone loss, the simultaneous observation of cirrus clouds and trace gases species related to ozone chemistry can furthermore contribute to an improved understanding of the ozone destruction mechanisms. On the other hand, when not considered in the retrieval process the effect of cirrus clouds on the limb spectra, mainly a broadband signal change outside of strong lines, introduces further uncertainty to retrieved trace gas profiles and the estimation of the background continuum around the UTLS. According to previous studies[13], a retrieval accuracy of better than 50 % is targeted for ozone in the upper troposphere, i.e., at altitudes where cirrus frequently occurs. Here, we evaluate the error budget on ozone that will be introduced by not considering cirrus when retrieving trace gases.

Focusing this study on the impact on retrieval from SMILES, a similar instrumental setup is used. The O_3 profile is retrieved from simulated SMILES Band-A observations between 4–70 km tangent altitude with a vertical spacing of 2 km. To reduce complexity, measurements are assumed to be monochromatic with an infinite field of view, i.e., no spectral instrumental functions and no antenna pattern are applied. Furthermore, the effect of the second side band is neglected.

2.2 Simulation of measurements

For this theoretical study, SMILES observations are simulated using the radiative transfer (RT) forward model SARTre[9]. SARTre has been designed for monochromatic high resolution RT modeling in the infrared spectral range and beyond for arbitrary viewing geometries in spherical atmospheres, taking emission as well as scattering into account as sources of radiation. Using the integral radiative transfer equation

$$I(\nu) = I_\mathrm{b}(\nu)\,e^{-\tau(\nu)} + \int_0^{\tau(\nu)} J(\tau',\nu)\,e^{-\tau'(\nu)}\,d\tau' \quad (1)$$

radiation sources are "collected" along the observer line of sight (LoS) and transmitted to the instrument following Beer's law. Here $I(\nu)$ is the monochromatic intensity at wavenumber ν reaching the observer, I_b denotes background radiation, e.g., emission of the cold space, and τ is the optical depth, measured from the observer along the LoS. The source term

$$J = J_\mathrm{B} + J_\mathrm{SS} + J_\mathrm{MS} \quad (2)$$

comprises thermal emission (B), single scattered solar radiation (SS), and multiple scattering (MS). The diffuse incident radiation field required for the calculation of the multiple scattering source J_MS is derived assuming a locally plane-parallel atmosphere and obtained using the pseudo-spherical version PSDISORT[2] of the radiative transfer solver DISORT[14].

According to CIWSIR Study Team[1], in the tropics approximately 10 % of the ice mass exists above 10 km, the altitude at which the atmosphere becomes opaque in the complete spectral region covered by the SMILES bands. Similar detection frequencies of ice mass fraction can be found in the midlatitudes, where cirrus clouds in general exist at lower altitudes, but where SMILES saturation altitudes also reach lower into the atmosphere due to lower water vapor content compared to the tropics. However, cirrus occurence is more frequent in the tropics, i.e., cirrus observations by SMILES will mainly take place in the tropics. Hence, cirrus impact is studied here on the basis of observations that are simulated using atmospheric setups, i.e., atmospheric profiles as well as cloud micro- and macrophysical characteristics, corresponding to tropical conditions.

For both the simulation of the observations by SARTre as well as in the retrieval by MOLIERE (see section **2.3**) an identical atmospheric setup is used except for the cirrus clouds. Therefore, profiles of temperature, pressure and trace gases representing tropical atmospheric scenario implemented in MOLIERE are used[11][15]. Moreover, mole-

cular absorption coefficients are pre-calculated by MOLIERE and applied in the forward calculation of SARTre in order to minimize additional error contributions from forward modeling uncertainties. All of the significantly interfering trace gases in the SMILES bands have been considered in the line-by-line calculation of the molecular absorption coefficients, i.e., H_2O, O_3, HCl, ClO, H_2O_2, $HOCl$, HNO_3, SO_2, BrO, HO_2, $OClO$ and CH_3CN.

A number of cirrus cloud scenarios has been evaluated with cirrus microphysical characteristics adopted from Liou[8], where ice water content (*IWC*) and particle size distribution (SD) are parameterized in terms of ambient temperature. For all cloud scenarios, single scattering properties of the cirrus particles where derived from Mie calculations assuming spherical particles consisting of pure ice. Furthermore, a SD with parametrization temperature of $T = -50°C$ has been applied, giving an effectice particle size for the particle bulk of $D_e = 42\,\mu m$. A "default" cloud case has been defined with cloud top altitude $z_{top} = 13$ km and $IWC = 2$ mg/m^3 according to $T = -50°C$, which results in a vertical ice water path of $IWP = 2$ g/m^2 for the 1 km thick cloud layer. Based on the "default" case, scenarios with *IWC* varied between 0.1 mg/m^3 and 40 mg/m^3 and z_{top} varied between 8–16 km are studied. A summary on scenario setup is given in Table 2 for the cases discussed in detail in this paper.

2.3 Error estimation and retrieval

Error estimation and O_3 profile retrieval is performed using MOLIERE[16]. MOLIERE is a clear-sky thermal emission radiative transfer forward and inversion model for arbitrary observation geometries in a spherical atmosphere. For inversion MOLIERE applies the Optimal Estimation Method according to Rodgers[12].

In order to minimize contributions from any other error sources except for the clouds themselves identical forward model parameters are used for the simulation of the observations by SARTre and for the retrieval by

Table 2 Definition of evaluated cloud cases

case name	IWC [mg/m^3]	z_{top} [km]
"default"	2.0	13.0
"thick"	40.0	13.0
"high"	2.0	16.0

MOLIERE. That is, instrumental configuration, observation geometry and all atmospheric profiles that are not retrieved are assumed to be perfectly known with the same trace gas species considered. Furthermore, *a priori* and first guess profiles of ozone are identical to the observed one. The error of the ozone *a priori* profile is set to 100 %. Both measurement and *a priori* covariances are assumed to be uncorrelated.

Beside O_3, retrieval of further parameters is evaluated concerning their suitability to account for the spectral effects of the cirrus. This in particular inludes the derivation of an offset and slope (zero and first order baseline, respectively) in brigthness temperature (*BT*) for each measured spectra as well as the retrieval of the water vapor profile. With no H_2O lines within the spectral region of SMILES band-A, water vapor is assumed to only contribute radiatively by continuum absorption and emission. Due to this spectral broadband behaviour, the retrieval of H_2O volume mixing ratio (*VMR*) can be interpreted as the derivation of a baseline in extinction coefficients, with the retrieved profile then being a "pseudo" water vapor *VMR* deviating from the true atmospheric H_2O profile. For *a priori* and first guess profiles of H_2O, the true profile is used with an *a priori* error of 100 %. *A priori* values for zero and first order baseline are 0.0 ± 5.0 K for zero order and 0.0 ± 1.0 K/GHz, respectively.

In addition to retrieving further items, control parameters of the inversion code might be used to support compensation of cloud effects. Here, setting an opacity limit and manipulating the random noise error of the measurement

are evaluated. Using the opacity limit parameter excludes all spectral channels from the inversion process, where clear-sky atmospheric opacity along the LoS exceeds the set limit. This is usually applied to avoid highly non-linear relations in the inversion process and to stabilize the solution. Changing the measurement error due to random noise manipulates the trust level that is given to the measurement. For non-manipulated measurement error, a value of approximately 0.5 K is set accoring to the random noise error of SMILES.

The error contributions on the retrieved profile are estimated using the relation

$$\hat{x} - x^{\mathrm{true}} = G \cdot (y_{\mathrm{obs}} - y^{\mathrm{true}}) + (I - A) \cdot \varepsilon_{\mathrm{a}} + G \cdot \varepsilon_{\mathrm{meas}}, \quad (3)$$

where $\hat{x}$ and x^{true} are the retrieved and the true profile, respectively, y_{obs} is the observation vector from SARTre and y^{true} contains the MOLIERE calculated spectra corresponding to the true profile x^{true}. ε_{a} and $\varepsilon_{\mathrm{meas}}$ are the errors of the *a priori* profile and of the measurement, respectively. G is gain matrix with

$$G = (K^T S_{\mathrm{y}}^{-1} K + S_{\mathrm{a}})^{-1} \cdot K^T S_{\mathrm{y}}^{-1}, \quad (4)$$

where S_{y} and S_{a} are the covariance matrices of the observations and of the *a priori* profile, respectively, and K is the weighting function matrix. In Eq. (3) I is the identity matrix and A the averaging kernel matrix defined as

$$A = G \cdot K. \quad (5)$$

The first term on the right hand side of Eq. (3) describes the error due to the observation, the second terms is the error due to the *a priori* (smoothing or null space error), and the third term gives the error contribution due to the measurement error (thermal noise). Since MOLIERE is a clear-sky model, weighting functions can only be derived assuming clear-sky conditions. For discussing effects of cirrus and evaluating the ability to retrieve trace gas profiles in case of clouds, weighting functions are derived from SARTre simulations using finite differences approach for clear-sky and cloudy conditions. Details are given and discussed in section **4**.

3 Cloud effects on observations

In general, clouds cause a decrease in intensity by extinction due to absorption and due to scattering of radiation out of the path. They increase intensity by emission and by scattering into a path. These processes happen simultaneously and in every case, but scattering is neglecteable, where molecular absorption and/or emission dominates, i.e., in the centers of strong absorption lines and bands. Furthermore, in contrast to molecular absorption and emission, cloud optical properties usually show broadband characteristics. Whether the total effect is an increase or a decrease in radiation compared to a cloud-free case, depends on a variety of parameters. Among these, cloud altitude and observation geometry play the key role in case of observations of longwave radiation.

Concerning sub-mm limb measurements most cloud cases result in decreased intensity or brightness temperature. An increase of radiation occurs only when a cloud is observed by a measurement with the tangent point in the uppermost troposphere. In these cases under clear-sky conditions the atmosphere is transparent until far behind the tangent point, i.e., a cold background is observed. The amount of radiation lost through extinction by the cloud is small, but the cloud emits radiation and scatters radiation originating from lower and warmer parts of the troposhere into the LoS. In case of lower tangent altitude measurements the background is much warmer, i.e., the effect of extinction is stronger than the scattering into the LoS. Cloud effects on SMILES band-A limb observations in the upper troposphere are illustrated in Fig. 1 and Fig. 2.

In the clear-sky spectra plot in Fig. 1, the O_3 line at 625.37 GHz can clearly be identified by its constantly high *BT*, that arises from the LoS being saturated in the ozone rich, warm region of the stratosphere. No radiation from the troposphere reaches the observer around the line center, hence clouds do not influence the observation there as can be seen

from the cloud effect plots of Fig. 1. In the uppermost troposphere and lower stratosphere, also an ensemble of HCl lines can be recognized around 624.98 GHz by slightly higher BT than in the spectral region around. Similar to ozone, the center region of these lines is not or to a weaker extent affected by clouds, which is due to the major fraction of the signal reaching the observer originating from above the cloud. Outside these lines, the clear-sky tropospheric spectra of SMILES band-A are dominated by continuum absorption and emission of water vapor. This is reflected in the strong increase of BT in the uppermost troposphere and the saturation for tangent altitudes $z_{tan} < 11$ km, where the atmosphere becomes opaque before the LoS reaches the tangent point (see, e.g., clear-sky BT profiles in Fig. 2.

The effect of cirrus in difference to clear-sky spectra is shown in the lower panel of Fig. 1 for the cirrus case we defined as "default" along with a cirrus of "high" altitude and a "thick" cirrus (see Tab. 2 for details on cloud scenario definitions). In contrast to ultraviolet to near-infrared limb observations, sub-mm measurements with tangent point

above the cloud are not influenced by the cloud due to the lack of scattering particles there. Hence, BT changes can only be observed when the LoS intersects the cloud, i.e., for observations with $z_{tan} < 16$ km for the "high" cloud case (Fig. 1, lower panel, right) and at $z_{tan} < 13$ km for the "default" and "thick" cloud cases (Fig. 1, lower panel, middle and left). Apart from the "high" cloud case, where the cloud enhances BT for tangent altitudes down to about 13 km, the cirrus decreases BT compared to the clear-sky case.

As shown in the left panel of Fig. 2, for thin and moderately thick clouds (like the "default" cloud) the decrease of BT compared to clear-sky BT is largest for the uppermost LoS observing the cloud and gets lower with lower tangent altitudes. This behaviour can be explained by the LoS path length through the cloud becoming shorter and therefore more transparent for lower tangent altitudes. Hence, a higher fraction of radiation originating from the lower and warmer troposphere can penetrate through the cloud. On the other hand, when the cirrus is thick and becomes opaque itself, the cloud induced negative BT changes
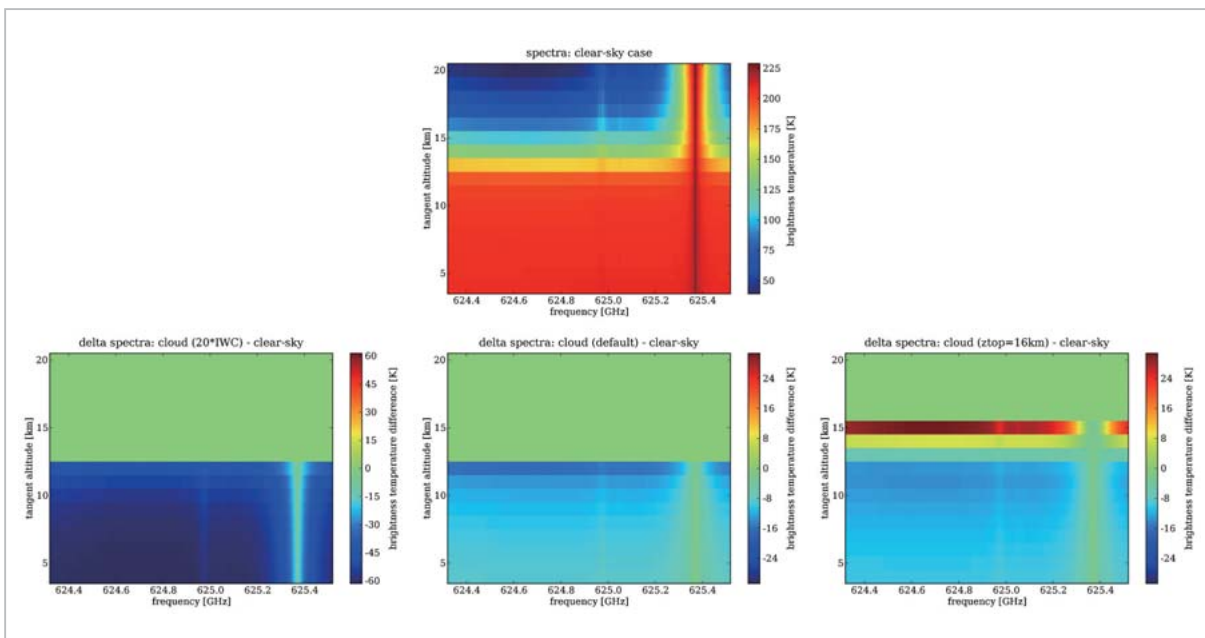

Fig.1 (top) Clear-sky brightness temperature spectra of tropospheric and lower stratospheric tangent altitude measurements. (bottom) BT differences to clear-sky spectra for (middle) "default" cirrus cloud (z_{top} = 13 km, IWC = 2 mg/m³), (left) the "thick" cirrus with larger ice content (IWC = 40 mg/m³), and (right) the "high" cirrus with raised cloud altitude (z_{top} = 16 km). For more details on the cloud case definitions see section 2.2
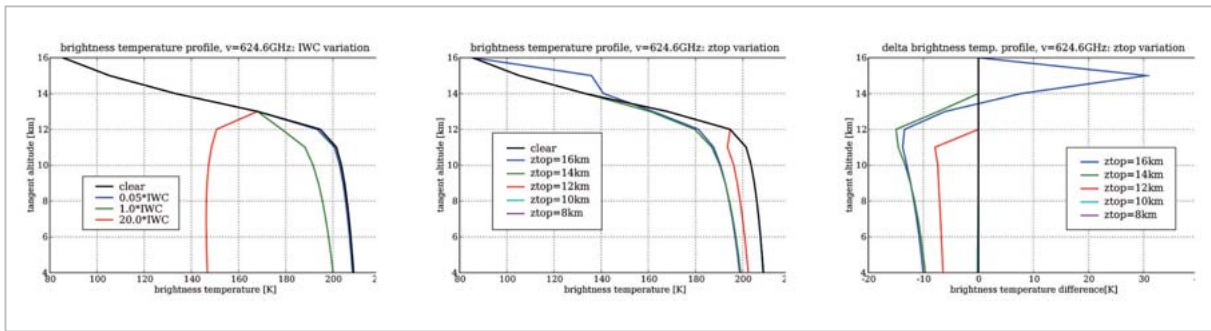
Fig.2 *(left) Brightness temperature profiles in SMILES band-A continnum region (v = 624.6 GHz) for cirrus with varied ice content ("default" cirrus IWC multiplied by 0.05, 1.0 and 20.0). (middle) Corresponding brightness temperature and (right) brightness temperature difference profiles for cirrus with varied cloud altitude*

increase with decreasing tangent altitude. Due to scattering effects absolute *BT* can even drop below cloud top black body temperature.

The pattern of moderately thick cirrus causing a *BT* decrease that gets lower with decreasing tangent altitude is found for clouds with top altitudes below approximately 14 km (see Fig. 2, middle and right panel). For these cirrus, cloud effects are the larger the higher cloud is, while effects of clouds with top altitutes below about 10 km are negligible because the atmosphere becomes opaque before the LoS intersects the cloud. Only in case of cirrus located in the uppermost troposhere, i.e., above 14 km, an increase of *BT* compared to clear-sky conditions can be observed for the upper tangent altitudes measuring the cloud. As discussed before, this is due to scattering into the LoS being larger than the extinction of the radiation originating from a transparent atmosphere, i.e., from a cold background. However, at lower tangent altitudes extinction effects dominate over emission and scattering into the LoS for these cloud cases as well. That means, cirrus affected limb *BT* are generally lower than clear-sky limb *BT* at middle and lower tropospheric tangent altitudes, i.e., tangent altitudes below approximately 13 km.

In summary, in the continuum regions of SMILES band-A *BT* enhancements as well as decreases of several tens of Kelvin can be caused by cirrus cloud. Even very thin cirrus (0.05*IWC case in Fig. 2, left panel, corresponding to *IWC* = 0.1 mg/m³) lead to broad-

band *BT* changes in the order of the instrumental thermal noise of SMILES of 0.5 K.

4 Weighting functions

Weighting functions, defined as $dI(v, z_{tan})/dx(z)$ with *x* being the retrieval parameter and *z* its location in altitude, for O_3, H_2O, and cloud ice water content have been calculated and evaluated in order to derive information about

(1) where — in spectral and spatial sense — the information in the retrieval is or can be taken from

(2) how strong this information is, in particular for ozone in relation to other high influence atmospheric parameters like water vapor and cirrus

(3) the changes of this information due to cirrus occurence in general and cirrus parameter changes in particular.

In summary, evaluating the weighting functions shall give a measure for the ability to retrieve atmospheric parameters, in particular O_3, and for their separability from the other parameters.

Like — to our knowledge — all inversion models used for trace gas retrievals, the calculation of analytic weighting functions by MOLIERE is restricted to clear-sky atmospheric conditions. Therefore, in this study weighting functions are derived using finite differences of forward modeling calculations by SARTre with perturbations of 1 % of the *VMR* or *IWC* at a single atmospheric level or

layer.

Figure 3 shows weighting functions with respect to O_3, H_2O and *IWC* for the tangent point layer, i.e., for $z_{tan} = z$, where the weighting functions are expected to be largest in case of limb observations. For O_3 and H_2O weighting functions for clear-sky conditions are presented along with their changes for different cloud cases. Weighting functions of *IWC* are given for a cirrus cloud in the particular retrieval layer and no cloud in the other layers above and below.

Because of the pressure dependence of the line shape function, in general maximum information about *VMR* of a certain trace gas at high altitude layers, where pressure is low and pressure broadening is weak, is to be derived from close to the line center, while intensity measurements from the line wings provides information about the atmospheric state at lower altitudes. That is, profile information for O_3, characterized by a strong line located within the SMILES band-A is concentrated in the center of the line for stratospheric layers and successively distributed towards the wings of the pressure broadened line in the tropospheric layers. However, due to the decreasing mixing ratio of O_3 and the growing importance of water vapor continuum absorption, absolute values of the weighting functions, i.e., information content of the observation, become very small even in higher layers of the troposphere (see Fig. 3, lefthand side, upper panel). In the uppermost troposphere at an altitude of 16 km a 100 % change in ozone *VMR* triggers a *BT* change of only about 1.5 K. Weighting functions indicate a three times larger *BT* change due to H_2O and *IWC* at this altitude, increasing to more than a magnitude at lower altitudes in the upper troposphere. Furthermore, both parameters show a much higher natural variability compared to O_3. From that it becomes obvious, that the retrieval of O_3 even in the uppermost troposphere is a very difficult task.

Spectral features of water vapor in SMILES band-A are mainly due to being placed in the wing of a strong H_2O line close
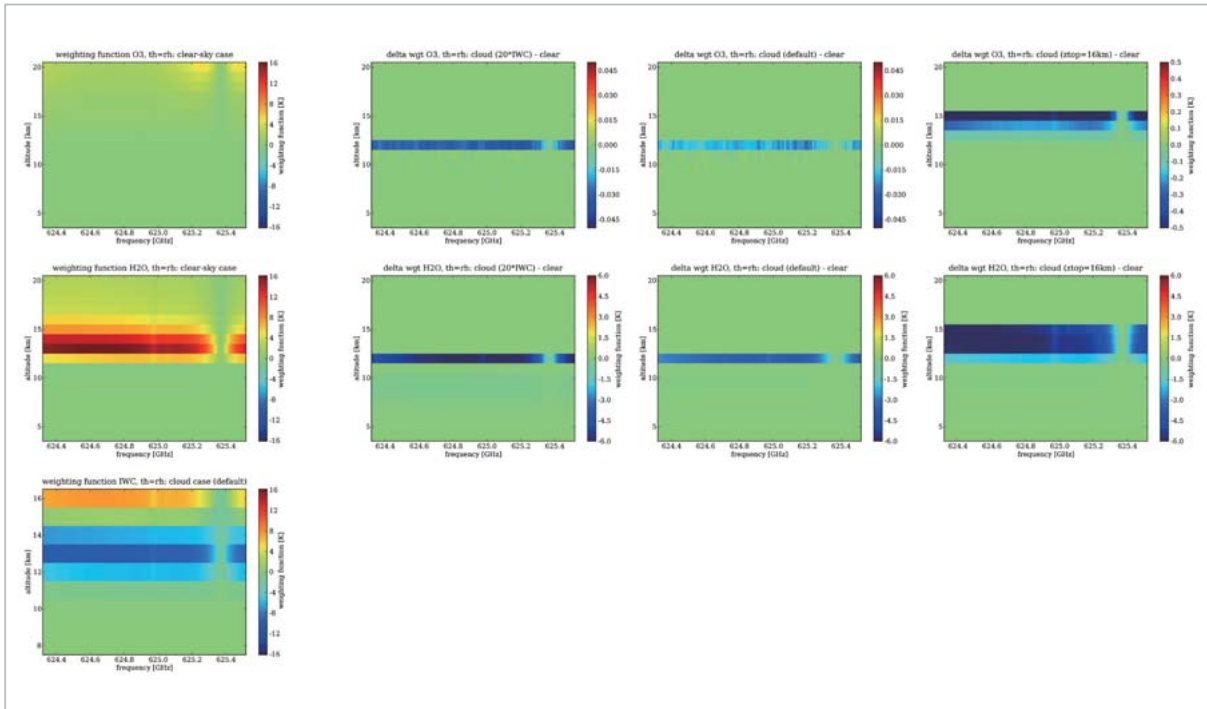

Fig.3 (left) Weighting functions of (top) O_3 and (middle) H_2O under clear-sky conditions and (bottom) cirrus IWC at the tangent point layer. IWC weighting functions are shown for the cloud only located in the tangent point layer and clear-sky conditions apply for all other layers. (right) Weighting function changes due to (from left to right) "thick", "default", and "high" cirrus for (top) O_3 and (middle) H_2O

to the band at 620.7 GHz. Hence, weighting functions of H_2O exhibit broad spectral tendencies overlaid by the effect of the O_3 line, around which the measurement saturates at stratospheric altitudes and tropospheric weighting functions are zero (see Fig. 3, middle panel, righthand side). Following the increasing water vapor content, weighting functions increase with decreasing altitude until 13 km. Below where the atmosphere is getting opaque and weighting functions drop rapidly below the measurement noise of SMILES at around 11 km.

As explained for O_3, pressure dependence of the line shape causes *VMR* information to be concentrated in the line centers for the high altitude layers and distrubuted over the wings towards lower atmospheric layers. That is, for H_2O with a line centered at 620.70 GHz spectral weighting functions of the stratospheric and uppermost tropospheric layers peak outside the lower frequency limit of the band and slowly decrease with frequency within the band. At $z = 13$ km weighting functions reach their maximum within the band. Lower layer spectral weighting functions increase with frequency in the band and peak outside the higher frequency band limit (see Fig. 4, left). This behaviour allows for retrieving humidity from SMILES band-A spectra, but is expected to disqualify the retrieval of pseudo water vapor *VMR* as extinction baseline to compensate for cirrus cloud effects.

Weighting functions of cirrus *IWC* (see Fig. 3, lower panel) emphasize the effects of cirrus discussed in section **3**:
- clouds at very high troposheric altitudes induce *BT* enhancements due to dominant scattering into the LoS
- effects of extinction on the one hand and emission / scattering into the LoS cancel out in subsequent atmospheric layers
- extinction dominates at altitudes, where the LoS becomes opaque around the tangent point, and *BT* decreases are observed.
- With the atmosphere getting opaque along the LoS within or before the cloud, sensitivity to cirrus diminishes and finally vanishes.

In the narrow spectral band of SMILES, cirrus bulk optical properties are basically constant. Therefore, *BT* changes due to cirrus itself would be spectrally flat, but are dominated by interferences from trace gases, in particular from O_3, HCl, and H_2O as illustrated in Fig. 3 (middle panel) and Fig. 4 (righthand side). In particular, for higher altitudes and outside the O_3 and HCl interfered regions, opposite weighting function tendencies are found for H_2O and *IWC*, i.e., where H_2O sensitivity decreases *IWC* weighting functions increase (for example compare weighting functions for altitude 15 km in left and right plots of Fig. 4). When cirrus *IWC* weighting functions are negative, the description and quantification of the interacting processes is more complex. However, it becomes apparent that the spectral behaviour of the H_2O and
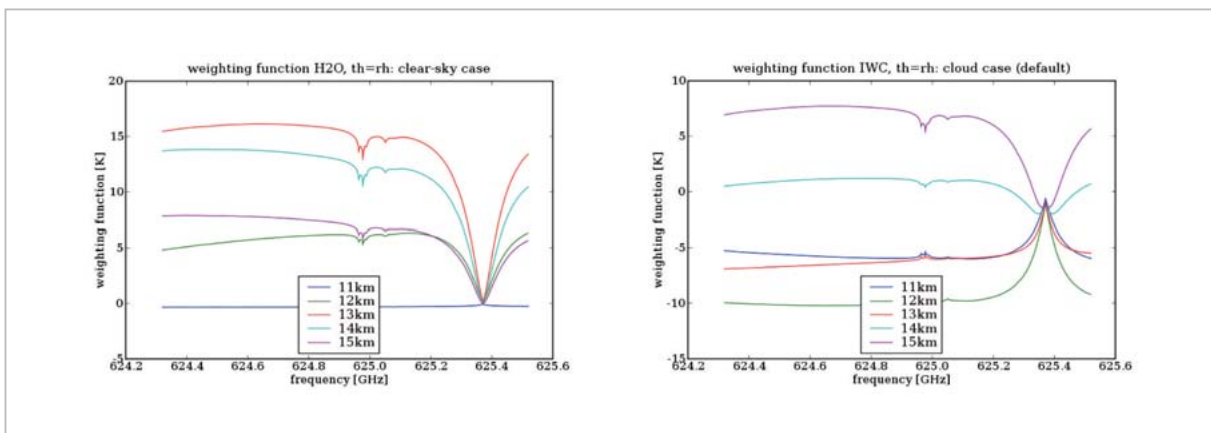

Fig.4 *(left) H_2O and (right) cirrus IWC weighting functions for selected $z_{tan} = z$*

IWC weighting function at the same altitudes differs. That means, a retrieval of a pseudo H_2O profile can not account for cirrus effects. On the other hand, this indicates that the effects of H_2O and *IWC* are separable and information about these parameters can be retrieced independently.

Beside the clear-sky weighting functions for O_3 and H_2O, their changes due to different cirrus clouds ("thick", "default", and "high" cirrus cases) are presented in the righthand side of Fig. 3. Changes in trace gas weighting functions for the three evaluated cloud conditions are basically restricted to the altitudes from cloud top down to the 12 km layer. In general, trace gas weighting functions, i.e., sensitivity of the measurement concerning trace gas *VMR*, decrease due to the cloud, with the loss being larger for the thicker as well as higher clouds. Nevertheless, for H_2O significant weighting function values are preserved in particular for high cirrus.

5 Error estimation and retrieval

The error budget in O_3 profile retrieval from SMILES band-A limb observations is derived based on Eq. (3) from a linear retrieval approach using the optimal estimation inversion model MOLIERE. Before estimating the error budget due to high altitude ice clouds, overall limitations of retrieval ability due to instrument setup and basic atmos-

pheric conditions are evaluated and the suitability of the simulation approach of the study is checked.

In Figure 5, left panel, O_3 averaging kernels (see Eq. (5)) are given along with the resulting measurement response. According to these, the observations are sensitive down to the 2 km thick layer centered around 11 km, when ozone is the only retrieved item. For the same setup, the *VMR* error contribution due to the *a priori* error (smoothing error) and due to the random thermal noise of the measurement (measurement error) are shown in comparison to the true O_3 profile in the right panel of Fig. 5. As indicated by the averaging kernels, the smoothing error is low down to the layer at 11 km. The error contribution of the random measurement noise is significantly lower than the O_3 mixing ratio for the layers at and above 13 km.

In addition, errors due to the observation are given for the clear-sky and the "default" cloud case. The further is derived performing a retrieval from SARTre simulated clear-sky condition measurements. By that, the uncertainty introduced by using different forward model codes is studied, i.e., the clear-sky observation error can be interpreted as the forward model error. The forward model uncertainty is at least one order of magnitude lower than the O_3 *VMR* above 15 km, but reaches 100 % at the 13 km layer. Differences between SARTre simulated observations and
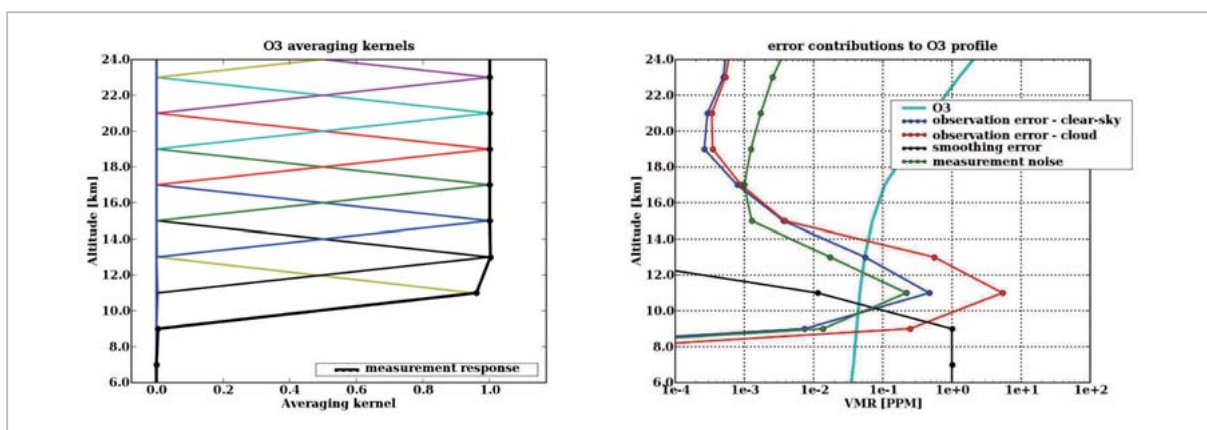

Fig.5 *(left) Averaging kernels and measurement response for O_3 profile retrieval. (right) Contributions of different error types to the total retrieval error (see Eq. (3)). The ozone profile is plotted for comparison*

MOLIERE modeled *BT* spectra of up to 1 K are found in the continuum regions of the SMILES band. This suggests that retrieval results are highly sensitive to small broadband signal changes below 14 km. Large retrieval errors have to be expected below this altitudes even in case of clear-sky conditions, i.e., a reliable retrieval of O_3 in the tropics is only possible in the uppermost troposheric layer.

5.1 Cloud induced retrieval errors

Error estimation results are presented in the left panel of Fig. 6. For comparison, observation error contribution of the clear-sky case as well as the true O_3 are given in adddition.

At the layer that contains the cloud as well as at subsequent lower layers, the observation error due to the "default" cloud is found about one order of magnitude larger than the forward model error. Beside that, the cirrus also causes slightly changed results for O_3 above the cloud top, which is due to the smoothing properties of the retrieval.

In addition to the effect of the "default" cirrus cloud, the impact of cirrus with varied ice water content is evaluated. Except from *IWC*, the properties of these cirrus clouds are identical to the ones of the "default" cloud.

It is found, that error contributions at the layer containing the cirrus and below are strongly enhanced compared to the clear-sky case. The relation between *IWC* and cloud observation error contribution to the derived profile is

approximately linear. It has to be noted, that even very thin cirrus of *IWC* = 0.1 mg/m³ and *IWP* = 0.1 g/m² gives a significantly larger error contribution than the forward model and induces errors larger than the O_3 *VMR*. As for the "default" cloud, results at layers above the cloud are slightly affected by the cirrus, but uncertainties remain very small.

5.2 Cloud compensation

In the previous subsection, the error budget has been estimated that is induced by not accounting for high altitude ice clouds in the retrieval of ozone profiles in the UTLS. Now we evaluate possibilities of accounting or compensating for cirrus clouds by means that are usually available in classical inversion models for atmospheric profile retrieval, i.e., models that do not consider clouds, in particular scattering ice clouds. As explained in section **2.3**, we study the suitability of deriving a *BT* baseline for each limb measurement and of retrieving a pseudo H_2O *VMR* profile that might serve as a baseline in extinction coefficients to compensate for cirrus effects. Furthermore, the ability of retrieval control parameters like setting an opacity limit for channels to be used in the retrieval as well as enhancing the measurement noise to stabilize the retrieval is evaluated. Results for the "default" cloud case based on linear mapping are given in the right panel of Fig. 6.
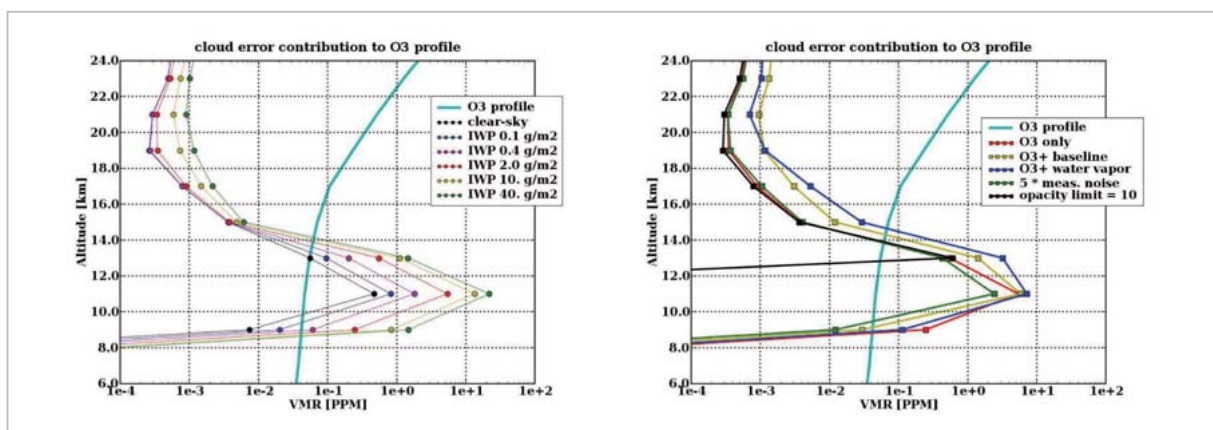
It is found, that setting an opacity limit

Fig.6 *(left) Cirrus cloud effect on retrieval by observation error contributions due to cirrus clouds of varied IWC. (right) Cirrus compensation suitability by observation error contributions of different retrieval setups. In each case, the true O_3 profile is plotted for comparison*

indeed stabilizes the solution at altitudes below 13 km, where the reliability of even clear-sky retrievals is not assured. In this sense, the usage of such a limit is suggested. But, since the inversion code does not know about clouds, this limit only applies to channels that become opaque under clear-sky conditions, i.e., no compensation for cirrus is possible. Furthermore, stabilizing the reliability of the retrieval is only done on the cost of losing any retrieval information from lower altitudes.

Manipulating the measurement noise relaxes the retrieval target in the sense, that it avoids the profile to be trimmed to fit the — probably cloud affected — observation very close. In the evaluated example, this parameter decreases the observation error contribution at altitudes below 13 km. On the other hand concerning total error of the retrieved profile this is balanced by a larger error contribution of the measurement error itself, that in particular will affect the quality of the profile at stratospheric layers.

The two additional retrieval parameters, baseline and pseudo H_2O, slightly improve the error contributions at the 9 km layer, but degrade results at all other altitudes compared to a pure O_3 retrieval. In particular, larger errors are induced at UTLS layers above the cloud. This behaviour is obvious for a *BT* baseline approach, that affects the whole spectrum in a similar way while cirrus has no or lower influence on *BT* at the center and wings of the O_3 line, respectively. Based on the evaluation of the weighting functions it has been expected, that a pseudo H_2O profile is not appropriate (see section **4**). With a strong line just outside the SMILES band-A, extinction coefficients of H_2O do not at all behave like a baseline but have significant line shape feature in the spectral region of interest. Furthermore, using another trace gas for extinction baseline reduces the degree of freedom of 2 (offset and slope) of a linear baseline to 1 (slope), controlled by the volume mixing ratio. That means, the findings for pseudo H_2O do not necessarily indicate the insuitability of an independently implemented real extinction

coefficient baseline. However, the ability of a pure extinction baseline to account for scattering effects of cirrus clouds is in question and needs to be evaluated. A more sophisticated alternative might be the application of a "grey body" extinction baseline, i.e., the determination of a factor accounting for extinction the mathematical unequal sign absorption/emission in case of scattering particles.

6 Conclusions

In this paper we have demonstrated effects of cirrus clouds on SMILES band-A spectra and their impact on ozone retrieval, when neither the cirrus is considered in the inversion nor the measurement excluded from the inversion. Furthermore, we evaluated weighting functions of ozone itself for clear-sky and cloudy conditions as well as those of water vapor and cloud ice water content.

As could be shown both from the evaluation of the weighting functions as well as from the error estimation, ozone profile retrievals from SMILES band-A are not reliable at altitudes below about 13 km even in case of clear-sky measurements. Although the "default" cloud case was defined to represent an average tropical cirrus, studying less frequently observable higher cirrus might give a more solid estimate about cloud impact on ozone retrieval. Nevertheless, it was shown, that retrieval of pseudo H_2O can not serve as an extinction baseline. On the other hand and apart from ozone retrieval, weighting functions were found to indicate that independent information about clouds and water vapor VMR can be derived in the upper troposphere.

In the future, we will study the suitability of retrieving an independent extinction baseline. Since ice clouds in limb observations do not act as black bodies [see, e.g.,[9]] and since it is basically impossible to model scattering effects by means of a black body assumption, i.e., absorption / emission = extinction[7], it furthermore seems worth to evaluate the suitability of a "grey body" extinction baseline. However, to ensure robustness in trace

gas retrievals, the detection and flagging of cloud affected spectra is advantageous. For SMILES observation setup this will be evaluated in further studies.

Acknowledgments

References

1 CIWSIR Study Team. Establishment of Mission and Instrument Requirements to Observe Cirrus Clouds at Sub-millimetre Wavelengths. Task 3 Report REP/PR131/008, ESA-ESTEC, 2006.

2 A. Dahlback and K. Stamnes, "A new spherical model for computing the radiation field available for photolysis and heating at twilight", Planet. Space Sci., 39 (5): 671-683, 1991.

3 C. Davis, C. Emde, and R. Harwood, "A 3D Polarized Reversed Monte Carlo Radiative Transfer Model for mm and sub-mm Passive Remote Sensing in Cloudy Atmospheres", IEEE T. Geosci. Remote, 43(6): 1096-1101, 2005.

4 M. Ekström, P. Eriksson, B. Rydberg, and D. Murtagh, "First Odin sub-mm retrievals in the tropical upper troposphere: humidity and cloud ice signals", Atmos. Chem. Phys., 7(2): 459-469, 2007.

5 C. Emde, S. Buehler, P. Eriksson, and T. Sreerekha, "The effect of cirrus clouds on microwave limb radiances", J. Atmos. Res., 72(1-4): 383-401, 2004. doi:10.1016/j.atmosres. 2004.03.023.

6 P. Eriksson, M. Ekström, B. Rydberg, and D. Murtagh, "First Odin sub-mm retrievals in the tropical upper troposphere: ice cloud properties", Atmos. Chem. Phys., 7(2): 471-483, 2007.

7 M. Höpfner, H. Oelhaf, G. Wetzel, F. Friedl-Vallon, A. Kleinert, A. Lengel, G. Maucher, H. Nordmeyer, N. Glatthor, G. Stiller, T. von Clarmann, H. Fischer, C. Kröger, and T. Deshler, "Evidence of scattering of tropospheric radiation by PSCs in mid-IR limb emission spectra: MIPAS-B observations and KOPRA simulations", Geophys. Res. Lett., 29(8): 119, 2002. doi: 10.1029/2001GL014443.

8 K. N. Liou, "Radiation and Cloud Processes in the Atmosphere", Oxford University Press, New York, 1992.

9 J. Mendrok, "The SARTre Model for Radiative Transfer in Spherical Atmospheres and its Application to the Derivation of Cirrus Cloud Properties", Ph.D thesis, Freie Universität Berlin, Germany, 2006.

10 D. Murtagh, U. Frisk, F. Merino, M. Ridal, A. Jonsson, J. Stegman, G. Witt, P. Eriksson, C. Jiménez, G. Mégie, J. de La Noë, P. Ricaud, P. Baron, J. Pardo, A. Hauchecorne, E. Llewellyn, D. Degenstein, R. Gattinger, N. Lloyd, W. Evans, I. McDade, C. Haley, C. Sioris, C. von Savigny, B. Solheim, J. McConnell, K. Strong, E. Richardson, G. Leppelmeier, E. Kyrölä, H. Auvinen, and L. Oikarinen, "An overview of the Odin atmospheric mission", Can. J. Phys., 80(4): 309-319, 2002.

11 W. J. Reburn, R. Siddans, B. J. Kerridge, S. A. Figure 6: (left) Cirrus cloud effect on retrieval by observation error contributions due to cirrus clouds of varied IWC. (right) Cirrus compensation suitability by observation error contributions of different retrieval setups. In each case, the true O_3 profile is plotted for comparison. Bühler, A. von Engeln, J. Urban, J. Wohlgemuth, K. Künzi, D. Feist, N. Kämpfer, and H. Czekala, "Study on upper troposphere / lower stratosphere sounding", Technical report, ESTEC / Contract No.12053/97/NL/CN, 1999.

12 C. D. Rodgers, "Inverse Methods for Atmospheric Sounding——Theory and Practise, volume 2 of Series on Atmospheric, Oceanic and Planetary Physics", World Scientific, 2000. ISBN-981-02-2740-X.

13 SMILES, 2002. JEM/SMILES mission plan. Tech. rep., Version 2.1, NASDA / CRL, November 15 2002. http://smiles.tksc.nasda.go.jp/document/indexe.html.

14 K. Stamnes, S. C. Tsay, W. Wiscombe, and K. Jayaweera, "Numerically stable algorithm for discrete-ordinate-method radiative transfer in multiple scattering and emitting layered media", Applied Optics, 27: 2502-2509, 1988.

15 J. Urban, "Retrieval of Species with Weak lines", In The Retrieval of Data from Sub-Millimetre Limb Sounding — CCN 2, chapter 2, pages 89-146. ESTEC/Contract No.11979/97/NL/CN-CCN2, September 2000b.

16 J. Urban, P. Baron, N. Lautié, K. Dassas, N. Schneider, P. Ricaud, and J. de La Noë, "Moliere (v 5): A versatile forward- and inversion model for the millimeter and sub-millimeter wavelength range", J. Quant. Spectrosc. Radiat. Transfer, 83(3-4):529-554, 2004a.

17 J. Waters, L. Froidevaux, R. Harwood, R. Jarnot, H. Pickett, W. Read, P. Siegel, R. Cofield, M. Filipiak, D. Flower, J. Holden, G. Lau, N. Livesey, G. Manney, H. Pumphrey, M. Santee, D. Wu, D. Cuddy, R. Lay, M. Loo, V. Perun, M. Schwartz, P. Stek, R. Thurstans, M. Boyles, K. Chandra, M. Chavez, G. S. C. B. Chudasama, R. Dodge, R. Fuller, M. Girard, J. Jiang, Y. Jiang, B. Knosp, R. LaBelle, J. Lam, K. Lee, D. Miller, J. Oswald, N. Patel, D. Pukala, O. Quintero, D. Scaff, W. Snyder, M. Tope, P. Wagner, and M. Walch, "The Earth Observing System Microwave Limb Sounder (EOS MLS) on the Aura satellite", IEEE Trans. Geosci. Remote Sens., 44(5): 1075-1092, 2006.

18 D. Wu, J. Jiang, and C. Davis, "EOS MLS cloud ice measurements and cloudy-sky radiative transfer model", IEEE Trans. Geosci. Remote Sens., 44(5): 1156-1165, 2006.

***Jana MENDROK**, Ph.D.*

Expert Researcher, Environment Sensing and Network Group, Applied Electromagnetic Research Center

Radiative Transfer Modeling and Cloud Remote Sensing

***Philippe BARON**, Ph.D.*

Guest Researcher, Environment Sensing and Network Group, Applied Electromagnetic Research Center

Development of Forward and Retrieval Models for Atmospheric Remote Sensing

***KASAI Yasuko**, Dr. Sci.*

Senior Researcher, Environment Sensing and Network Group, Applied Electromagnetic Research Center

Spectroscopic Remote Sensing of Atmosphere